ELSEVIER

Journal of Organometallic Chemistry 557 (1998) 187–205

Journal of Organometallic Chemistry

Tin(IV) and organotin(IV) derivatives of novel β-diketones. III[1] Diorgano- and dihalotin(IV) complexes of 1,3-dimethyl-4-R(C=O)-pyrazol-5-one (R = CH_3, C_6H_5) and the crystal structure of *trans*-dicyclohexylbis(1,3-dimethyl-4-acetylpyrazolon-5-ato)tin(IV)

C. Pettinari [a,*], F. Marchetti [a], A. Cingolani [a], D. Leonesi [a], E. Mundorff [b], M. Rossi [b], F. Caruso [c]

[a] *Dipartimento di Scienze Chimiche, Università degli Studi, via S. Agostino 1, 62032 Camerino, Macerata, Italy*
[b] *Vassar College, Department of Chemistry, Poughkeepsie, NY 12604-0484, USA*
[c] *Istituto di Strutturistica Chimica 'G. Giacomello', CNR, CP 10, 00016, Monterotondo Stazione, Roma, Italy*

Received 18 July 1997; received in revised form 6 October 1997

Abstract

Several diorgano- and dihalotin(IV) derivatives of new β-diketonate donors, 1,3-dimethyl-4-R(C=O)pyrazol-5-ones (R = Me, Q_DH; R = Ph, Q_MH) have been synthesized and characterized with analytical and spectroscopic methods. They are stable monomeric species, very soluble not only in aromatic and chlorohydrocarbon solvents, but also in alcohols and hydroalcoholic solutions. In the solid state, the diorganotin(IV) derivatives adopt a skewed trapezoidal bipyramidal geometry. The X-ray structure of bis(1,3-dimethyl-4-acetylpyrazolon-5-ato)dicyclohexyltin(IV) shows marked distortion of the organometallic C–Sn–C angle (155°) and two different sets of Sn–O distances. The factors affecting the distortion of this type of complex are discussed. The dihalotin(IV) derivatives $(Q)_2SnX_2$ (X = F, Cl, Br and I) are likely *cis* octahedral in the solid state, whereas in solution they exist as a mixture of *cis* and *trans* isomers. ^{119}Sn-NMR solution data are discussed and related to electronic and steric properties of the β-diketonate donor, and also to the nature of the halo and organic groups bound to tin.

Keywords: Tin(IV) complexes; 4-Acyl-5-pyrazolones; Crystal structure; IR; NMR

1. Introduction

A few years ago we initiated the investigation on the interaction between organotin(IV) acceptors and a class of β-diketonate ligands [1], 4-acyl-5-pyrazolones (QH), which possess the chelating moiety fused with a pyrazole ring (Fig. 1).

These molecules are currently used as metal extractants [2] and dyes [3], and they have recently shown interesting coordination behavior with several metal ions [4].

With several of these asymmetric donors we have obtained $(Q)_2SnR_2$ derivatives having structural and chemical properties clearly different from the analogous acetylacetonato–tin(IV) complexes [5]. Several of these complexes show X-ray crystal structures with strongly distorted octahedral geometries around tin and two different sets of Sn–O distances and a C–Sn–C angle smaller than 180° [6]. Also these structures always show a short C–H···O contact between the carbonyl (5 position) oxygen of the pyrazole ring and the ortho C–H in the R^1 phenyl (Fig. 2).

* Corresponding author.

[1] Part II is ref. ([6]e)

0022-328X/98/$19.00
PII S0022-328X(97)00680-3

As predicted by Kepert in his theoretical model [7], an increase in octahedral distortion is accompained by a reduction of the ligand bite angle O_s–Sn–O_p (where O_s/O_p stands for oxygen atoms associated to secondary/primary Sn–O bonds). This feature can be ascribed to two factors: the type of organic groups bonded to tin and the type of substituents R^1, R^2 and R^3 in the ligand. So far we have investigated the modification in the 4-acyl moiety (R^3), because of easier synthetic routes and, in fact, the literature reports only ligands having different R^3 groups, with $R^1 = Ph$ and $R^2 = Me$ [8].

In this report we describe the synthesis of two novel ligands, Q_DH ($R^1 = R^2 = R^3 = Me$) and Q_MH ($R^1 = R^2 = Me$ and $R^3 = Ph$) (see Fig. 1). For $R^1 = Me$ the previously mentioned C–H···O contact is eliminated and so one factor that can potentially contribute to the octahedral distortion is avoided.

The ligand Q_DH can be regarded as the simplest in the family of 4-acyl-5-pyrazolones and the most similar to acetylacetone or 2,4-pentanedione (acacH). It is interesting to note that acacH (the first ligand to be used as a complexing agent) is the prototype of β-diketonate donors, whereas Q_DH has now been synthesized by us, about 30 years after 1-phenyl-3-methyl-4-benzoyl-5-pyrazolone (Q′H) (Fig. 1), which can be regarded as the prototype of acylpyrazolones [9].

The ligand Q_MH is a structural isomer of the previously employed 1-phenyl-3-methyl-4-acetyl-5-pyrazolone (Q″H) (Fig. 1) ([1,6]c) from which it differs only by the inversion of one Me with a Ph group in R^1 and R^3 positions.

These donors are markedly different with respect to the previously employed 4-acyl-5-pyrazolones. They show good solubility not only in several organic solvents, as did previous ligands, but also in alcohols and water: a very important property in view of the possible biological applications of their $R_2Sn(IV)$ and $X_2Sn(IV)$ derivatives. In fact, several related tin(IV) compounds are known to possess in vitro antitumoral activity, comparable to that of Cisplatin [10]. It is believed that the ligand behaves as a carrier of the R_2Sn^{2+} moiety through cell membranes to allow interaction with the target cell. The mechanism by which these compounds exert their antitumor action is not known. Two factors concur to make their formulation as drugs difficult: the high cytotoxicity and insolubility in physiological media [11].

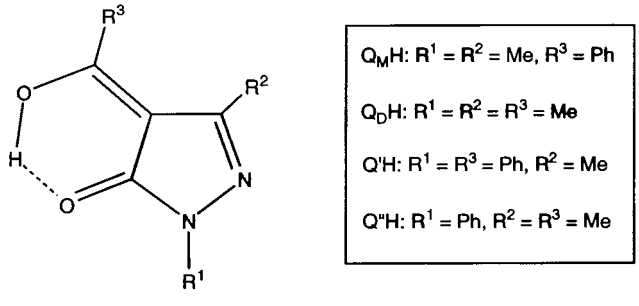

Fig. 1. 4-Acyl-5-pyrazolone proligands.

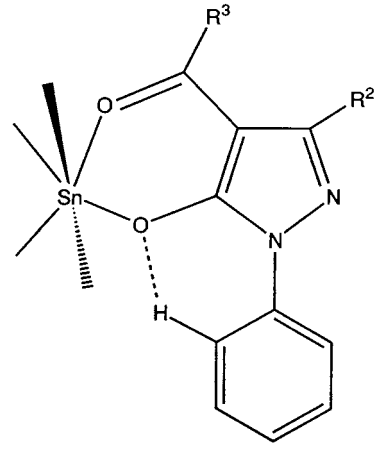

Fig. 2. The intramolecular O···H interaction.

The synthesis of several $(Q)_2SnR_2$ derivatives (R = Me, Et, Bu^n, Bu^t, Cy, Bz, Ph, F, Cl, Br and I), together with a study of their analytical, spectroscopic and structural features in the solid state and in solution are reported. The X-ray crystal structure of a dicyclohexyltin(IV) derivative provides additional information about the particular mode of action of these donors.

We also report here the synthesis and characterization of novel dihalotin(IV) derivatives $(Q)_2SnX_2$ (Q = Q′ and Q″; X = F, Cl, Br and I).

2. Results and discussion

Derivatives **1**, **3–8**, **10–15**, **17**, **20** and **25** have been synthesized as reported in Eq. (1):

$$2QH + 2KOH + R_nSnX_{4-n} \xrightarrow{MeOH} (Q)_2R_nSnX_{2-n} + 2KX + 2H_2O (QH = Q_MH, Q_DH, Q''H; R = Me, Et, Bu^t, Cy, Bz, Ph, Cl, Br; n = 0, 1, 2) \quad (1)$$

Derivatives **2** and **9** have been obtained in the following way:

$$2QH + Bu^n_2SnO \xrightarrow{Benzene,\ \Delta} (Q)_2SnBu^n_2 + H_2O \times (QH = Q_MH, Q_DH) \quad (2)$$

Derivatives **16**, **19**, **22** and **24** have been obtained in the following way:

$$2QH + SnF_4 \xrightarrow{CHCl_3,\ \Delta} (Q)_2SnF_2 + 2HF \times (QH = Q_MH, Q_DH, Q''H, Q'H) \quad (3)$$

Derivatives **18**, **21**, **23** and **26** have been obtained by halogen exchange of the corresponding dichlorotin(IV) complexes treated with a large excess of sodium iodide:

$$(Q)_2SnCl_2 + 2NaI \overset{THF,\ \Delta}{\rightarrow} (Q)_2SnI_2 + 2NaCl$$
$$\times (QH = Q_MH,\ Q_DH,\ Q''H,\ Q'H) \quad (4)$$

Dibromo and diiodotin(IV) derivatives $(Q)_2SnX_2$ (X = Br or I) can be obtained also by oxidative addition of X_2 to $(Q)_2Sn(II)$ [12]:

$$(Q)_2Sn(II) + X_2 \overset{CH_2Cl_2,\ h\nu/\Delta}{\rightarrow} (Q)_2SnX_2 \quad (5)$$

Analytical data are reported in Table 1.

Because $(Q_M)^-$ and $(Q_D)^-$ derivatives have high or medium solubility in most common solvents, it is more difficult to isolate and purify their complexes with respect to previously synthesized $(Q)_2SnR_2$ which have more hindered $(Q)^-$ donors. In fact, this type of compound is generally insoluble in polar protic solvents and precipitates from the alcoholic reaction solution, whereas compounds **1–20** show high solubility in alcohol and also in hydroalcoholic solutions. The latter are colloidal type solutions.

This particular physical property can be attributed to the ligands $(Q_M)^-$ and $(Q_D)^-$. In fact, the proligands Q_MH and Q_DH possess good solubility in water, probably due to H-interactions among H_2O molecules and the carbonylic O atoms and/or the N(2) atom (see later Fig. 8). This interaction seems not possible when the N(1) environment involves hindered or lipophilic groups such as a phenyl and so the solubility in protic solvents decreases.

2.1. Conductivity and molecular weight data

Derivatives **1–26** are non-electrolytes in dichloromethane. Moreover, the osmometric molecular weight determinations (Table 1), carried out in chloroform for several compounds, indicate a stable covalent mononuclear species in solution, thus excluding any dissociative equilibrium.

2.2. Infrared data

IR and far-IR data reported in Table 2 provide information about the nature of the donor–acceptor interaction. Assignments have been made on the basis of the literature available for dihalotin(IV) and diorganobis(β-diketonate)tin(IV) derivatives.

Comparing the spectra of the neutral proligands QH and those of compounds **1–26** the disappearance of the broad band between 3200 and 2700 cm^{-1} can be noted. This is due to the loss of the enolic proton upon complexation and so, an absence of the O–H···O intramolecular interaction.

It is known that β-diketones generally exist as a mixture of diketonic and keto-enolic tautomers. The neutral Q_DH ligand shows the first carbonyl band at 1680 cm^{-1}, whereas for Q_MH the value is 1630 cm^{-1}, therefore there is more diketonic form in Q_DH than in Q_MH.

The shift towards lower frequencies of the ν(C=O) indicates strong coordination of the ligand in the monoanionic form through both the carbonylic oxygens. In the region 470–390 cm^{-1} we have observed two or more strong absorptions, which have been assigned to ν(Sn–O) stretching [13]. The appearance of several Sn-O bands is likely due to the presence of different Sn–O bond distances (see diffraction study below). These absorptions also appear at higher frequencies (about 10–20 cm^{-1}) with respect to those of the previously synthesized $(Q)_2SnR_2$ compounds [1,6], thus indicating a stronger donor–acceptor interaction.

In the region below 650 cm^{-1} we assign other bands to ν(Sn–C) stretching modes [14]. In the case of Me, Et, Bu^n, Bz and Ph groups bonded to tin, well-distinguished strong or medium absorptions are found, but in the case of derivatives containing Cy and Bu^t groups the assignements are not certain, due to the presence of Sn–O and donor bands in the same area.

The absorptions due to Sn–X (X = F, Cl, Br, I) are observed at very different frequencies (Fig. 3).

In the spectra of **16**, **19**, **22** and **24**, the ν(Sn–F) are found at 580–560 cm^{-1} as one or two medium absorptions ([14]b). For the *cis* isomer, both symmetric and asymmetric Sn–F stretching modes are IR active. Also in the spectra of **15**, and of the other $(Q)_2SnCl_2$ derivatives (where Q = Q_M, Q′ and Q″) [1,6] the ν(Sn–Cl) fall at 350–330 cm^{-1} as two broad and intense peaks, indicating the presence of *cis* isomers in the solid state. Whereas in the spectra of **17**, **20**, **25** and $(Q')_2SnBr_2$ [12], the ν(Sn–Br) fall at 250–200 cm^{-1} and, in these cases, there are two or more strong bands. Finally, also diiodotin(IV) derivatives **18**, **21**, **23** and **26** show two or more strong absorbances due to ν(Sn–I) at about 200–220 cm^{-1}. Therefore, for dibromo- and diiodotin(IV) compounds we cannot exclude the presence of both *cis* and *trans* isomers in the solid state.

In addition, the ν(Sn–O) also are influenced by the type of halogens bonded to tin. In fact, these occur at higher frequencies in the presence of fluorine atoms, whereas they occur at lower frequencies in diiodotin(IV) derivatives. The $\sim$10 cm^{-1} increase in frequency of these bands on going from $(Q)_2SnI_2$ to $(Q)_2SnF_2$ can be interpreted in terms of the inductive effect of the increasing electron withdrawing power of the corresponding halogens, which strengthens the Sn–O bonds. Another explanation could be based on the variation in mass of the SnX_2 group to which the oxygens are linked in the series $(Q)_2SnX_2$.

This effect provides further support to our assignment of the 450 cm^{-1} bands to Sn–O stretching modes.

Table 1
Analytical data of compounds **1–26**

Compound (empirical formula)	No.	M.p. (°C)	Yield (%)	Elemental analyses[a]			F.W.	M.W.[b]	Conc.[c]	r[d]
				C	H	N				
$(Q_M)_2SnEt_2$	**1**	167–170	58	55.3	5.5	9.3	607	476	1.0×10^{-2}	0.78
$C_{28}H_{32}N_4O_4Sn$				(55.4)	(5.3)	(9.2)		508	2.0×10^{-2}	0.84
$(Q_M)_2SnBu^n_2$	**2**	83–85	85	57.7	6.3	8.4	663	519	1.1×10^{-2}	0.78
$C_{32}H_{40}N_4O_4Sn$				(57.9)	(6.1)	(8.4)		608	2.2×10^{-2}	0.92
								570	0.6×10^{-2}	0.86
$(Q_M)_2SnBu^i_2$	**3**	242–244	71	57.7	6.0	8.3				
$C_{32}H_{40}N_4O_4Sn$				(57.9)	(6.1)	(8.4)				
$(Q_M)_2SnCy_2$	**4**	137–140	66	60.1	6.4	7.7				
$C_{36}H_{44}N_4O_4Sn$				(60.4)	(6.2)	(7.8)				
$(Q_M)_2SnBz_2$	**5**	65–69	44	62.2	4.8	7.5	731	636	0.9×10^{-3}	0.87
$C_{38}H_{36}N_4O_4Sn$				(62.4)	(4.9)	(7.7)		649	1.8×10^{-2}	0.89
$(Q_M)_2SnPh_2$	**6**	104–108	78	62.3	4.5	7.9				
$C_{36}H_{32}N_4O_4Sn$				(61.5)	(4.6)	(8.0)				
$(Q_D)_2SnMe_2$	**7**	220–221	74	42.5	5.5	12.0	455	476	1.8×10^{-2}	1.05
$C_{16}H_{24}N_4O_4Sn$				(42.3)	(5.3)	(12.3)		455	1.0×10^{-2}	1.00
$(Q_D)_2SnEt_2$	**8**	178–181	70	45.0	6.3	11.2				
$C_{18}H_{28}N_4O_4Sn$				(44.8)	(5.8)	(11.6)				
$(Q_D)_2SnBu^n_2$	**9**	76–77	64	48.7	6.8	10.2				
$C_{22}H_{36}N_4O_4Sn$				(49.0)	(6.7)	(10.4)				
$(Q_D)_2SnBu^i_2$	**10**	191–192	68	48.1	6.9	10.2	539	556	1.0×10^{-2}	1.03
$C_{22}H_{36}N_4O_4Sn$				(49.0)	(6.7)	(10.4)				
$(Q_D)_2SnCy_2$	**11**	145–147	76	55.6	5.5	9.3	591	537	1.0×10^{-2}	0.91
$C_{26}H_{40}N_4O_4Sn$				(55.4)	(5.3)	(9.2)		498	1.8×10^{-2}	0.84
$(Q_D)_2SnBz_2$	**12**	177–179	58	55.0	5.5	8.9	607	509	0.9×10^{-2}	0.84
$C_{28}H_{32}N_4O_4Sn$				(55.4)	(5.3)	(9.2)		500	0.9×10^{-2}	0.82
$(Q_D)_2SnPh_2$	**13**	205–208	80	54.1	5.0	9.4	579	556	1.1×10^{-2}	0.96
$C_{26}H_{28}N_4O_4Sn$				(53.9)	(4.9)	(9.6)		493	1.8×10^{-2}	0.85
$(Q_D)_2SnMeCl$	**14**	209–211	54	38.1	4.5	11.5				
$C_{15}H_{21}ClN_4O_4Sn$				(37.9)	(4.4)	(11.9)				
$(Q_D)_2SnCl_2$	**15**	102–105	75	34.1	3.9	11.1				
$C_{14}H_{18}Cl_2N_4O_4Sn$				(33.9)	(3.7)	(11.3)				
$(Q_D)_2SnF_2$	**16**	195–200	54	36.6	4.0	12.0				
$C_{14}H_{18}F_2N_4O_4Sn$				(36.3)	(3.9)	(12.1)				
$(Q_D)_2SnBr_2$	**17**	234–239	63	28.5	3.2	9.4				
$C_{14}H_{18}Br_2N_4O_4Sn$				(28.7)	(3.1)	(9.6)				
$(Q_D)_2SnI_2$	**18**	280dec	55	24.5	2.8	8.2				
$C_{14}H_{18}I_2N_4O_4Sn$				(24.8)	(2.7)	(8.2)				
$(Q_M)_2SnF_2$	**19**	128–131	84	49.3	3.9	9.5				
$C_{24}H_{22}F_2N_4O_4Sn$				(49.1)	(3.8)	(9.5)				
$(Q_M)_2SnBr_2$	**20**	140dec	74	40.5	3.1	8.0				
$C_{24}H_{22}Br_2N_4O_4Sn$				(40.7)	(3.1)	(7.9)				
$(Q_M)_2SnI_2$	**21**	240dec	68	35.8	2.9	7.1				
$C_{24}H_{22}I_2N_4O_4Sn$				(35.9)	(2.8)	(7.0)				
$(Q')_2SnF_2$	**22**	252–254	74	57.2	3.8	7.8				
$C_{34}H_{26}F_2N_4O_4Sn$				(57.4)	(3.7)	(7.9)				
$(Q')_2SnI_2$	**23**	222–225	58	44.1	2.9	6.1				
$C_{34}H_{26}I_2N_4O_4Sn$				(44.0)	(2.8)	(6.0)				
$(Q'')_2SnF_2$	**24**	265–268	83	49.0	3.9	9.3				
$C_{24}H_{22}F_2N_4O_4Sn$				(49.1)	(3.8)	(9.5)				
$(Q'')_2SnBr_2$	**25**	240–242	75	40.7	3.2	7.8				
$C_{24}H_{22}Br_2N_4O_4Sn$				(40.7)	(3.1)	(7.9)				
$(Q'')_2SnI_2$	**26**	227–228	42	35.7	2.0	7.0				
$C_{24}H_{22}I_2N_4O_4Sn$				(35.9)	(2.8)	(7.0)				

[a] Values calculated in parentheses.
[b] Molecular weight determined osmometrically in chloroform solution at 40°C.
[c] Concentrations are in mol per 1000 g of solvent.
[d] r = M.W./F.W.

Table 2
IR data (nujol mull) of compounds **1–26**

No.	Compound	1700–1500 cm^{-1}	Sn–O	Sn–C	Sn–X[a]	<650 cm^{-1}
	Q_MH	1632sbr,1620s 1613sbr,1573s 1566s,1559s 1536s,1513m 1503m				615s,580s,553w 520m,458w,426s 408m,378s,338m 285s,270m,189s
1	$(Q_M)_2SnEt_2$	1600s,1593sh 1574m,1557sh 1523s,1498s	460m 408s 392s	550m		637w,627w,605s 533s,362m,302m 275w,256w,212m
2	$(Q_M)_2SnBu^n_2$	1600sh,1592s 1570s,1556sh 1527m,1497s	461m 404m 390vs	535s		647w,630w,605vs 580w,368m,302m 286w,266w,255m 209s,181s
3	$(Q_M)_2SnBu^t_2$	1598vs,1589s 1574s,1558m 1539sh,1532s 1527sh,1505m	462m 400m 393s	380s		551w,540sh,531s 369s,294s,280sh 260m,229m,169s 153m
4	$(Q_M)_2SnCy_2$	1595sh,1584s 1565vs,1557sh 1522s,1496m	461m 401m 390vs	535m 528m		643m,628m,602vs 371m,338m,317m 300m,279w,265m 216m
5	$(Q_M)_2SnBz_2$	1597sh,1585vs 1573s,1568s 1557m,1537m 1524br,1504s	455vs 408s 395sh	532s		640m,629m,601s 554w,418m,368m 303s,280w,268w 248m,226m
6	$(Q_M)_2SnPh_2$	1602s,1586s 1574s,1557sh 1525sh,1520s 1504s	460s 409m 233m	266s 245m		642w,630w,605s 537s,443s,426s 368m,307m,219w 206w,191w,165m
	Q_DH	1686s,1628sbr 1584s,1520s 1506sh				620s,598m,575s 552w,454w,425s 397m,329s,280w 243m,251s,203w 195m
7	$(Q_D)_2SnMe_2$	1601sbr,1575s 1557m,1526s 1505s	456s 419m 398m	586s		639s,615m,598s 552w,374m,368m 353w,326w,303m 280s,253m,247s 222m,202s,177s 151s
8	$(Q_D)_2SnEt_2$	1598sbr,1557sh 1527s,1501m 370m	457s 421m	551s		642m,625w,606s 499w,351w,291s 268w,220m,165sbr
9	$(Q_D)_2SnBu^n_2$	1605sh,1592vs 1557sh,1530m 1487m	458s 412s 406s	603sbr 510w		631s,495w,368m 351w,289m,262w 247w,201m 393m
10	$(Q_D)_2SnBu^t_2$	1592sbr,1575s 1557sh,1531m 1505m	457sbr 406m 392s	376m		633s,605s,551w 495w,351w,292s 263m,225w,201m 170sbr
11	$(Q_D)_2SnCy_2$	1595sbr,1577s 1558s,1526s 1506s	459m 408sbr	501w 490w		631s,606s,552w 374m,352w,341w 326m,291w,280m 267m,252w,224m 187vs,169sh,151s
12	$(Q_D)_2SnBz_2$	1599vs,1583s 1575s,1557s 1538s,1531sh 1504s	458s 415sbr	554m		631s,604s,501w 489w,340m,327m 289s,268s,225w 179sbr,155w
13	$(Q_D)_2SnPh_2$	1598s,1587s 1556s,1539m 1528s,1502m	464sbr 435sbr	277s 244s		643m,623w,605m 553m,373s,291m 205w,179m

Table 2 (continued)

No.	Compound	1700–1500 cm^{-1}	Sn–O	Sn–C	Sn–X[a]	<650 cm^{-1}
14	$(Q_D)_2SnMeCl$	1597sbr,1574s 1532s,1505s 447s	471s 454sh	541s	303sbr	643m,619m,603s 371s,274s,217m 203m,187s
15	$(Q_D)_2SnCl_2$	1602s,1574sbr 1534m,1508s 302m	463vsbr 330vs		338sh	619m,604vs,553w 374s,269m,203sh 197s,169m,159m
16	$(Q_D)_2SnF_2$	1601s,1582s 1574s,1537s 1514s	473vsbr 440sh		588s 576s	620sh,605s,555sh 377m,342w,298w 267w,228mbr,178sh
17	$(Q_D)_2SnBr_2$	1598s,1578vs 1533m,1506sh 458s 228m	471sh 463s 234m		253m 246vs	615m,604s,552m 542sh,419w,398w 376m,354w,324w 302w,290w,280m 265w,203w,171m 151s
18	$(Q_D)_2SnI_2$	1593vsbr, 1575sh 15232m, 1504m	470sh 454s		221sbr 204sh	618sh,603s,552w 372m,296m,268m 138m
19	$(Q_M)_2SnF_2$	1597s,1583s 1568s,1512vs	468sbr		588mbr	641w,629m,604s 551s,510w,373m 311m,267sh,239sbr 188sh
20	$(Q_M)_2SnBr_2$	1590sbr,1580sh 1573s,1567vs 1558s,1523s	464sh 455s		247vs 235sh	640w,628m,603s 549s,370w,334sh 315m,152m 1510sh,1504s
21	$(Q_M)_2SnI_2$	1591s,1578s 1558m,1525m 1505m	467m 452s		222s 202s	640w,629m,603s 544s,370w,314m 260m
22	$(Q')_2SnF_2$	1599s,1558s 1537s,1504s 450m	475s 468s		592s 588sh	645w,622m,618w 554s,506m,398w 355m,335m,289w 280w,245m,227s 202w,151m
23	$(Q')_2SnI_2$	1594s,1581s 1560vs,1540s 1525s	452s 443sh 432m		234sh 225vs 206s 199sh	643w,622s,611m 555s,515m,502m 468w,406w,382w 352m,337m,324m 300w,249m,187w
24	$(Q'')_2SnF_2$	1601s,1592s 1574s,1538s 1504m	489s 410m		595m 582vs	646w,622m,612m 563m,512m,394m 358w,333m,303w 279w,267w,252s 227w,214m,181w 151m
25	$(Q'')_2SnBr_2$	1595sbr,1554s 1514sbr	485s 403m		234vsbr	644w,625s,612s 582w,552w,511s 390sh,353w,329w, 308m,277m,202w 171m,151w
26	$(Q'')_2SnI_2$	1597s,1556s 1538s,1503s	472sh 460s 404m		223s 217sh 208s	642w,620s,611s 582w,553w,509s 391m,354w,328m 303m,276m,245w 183w,151w

[a] X = F, Cl, Br or I.

2.3. NMR data

The NMR data of the ligands and of compounds **1–26** are reported in Table 3 (^1H), Table 4 (^{13}C) and Table 5 (^{119}Sn).

In the ^1H-NMR spectra of the complexes $(Q)_2SnR_2$ and $(Q)_2SnX_2$ an upfield shift of the hydrogens in the R^1, R^2 and R^3 groups is generally observed. In the ^{13}C-NMR spectra two trends are observed, in agreement with those previously reported for analogues

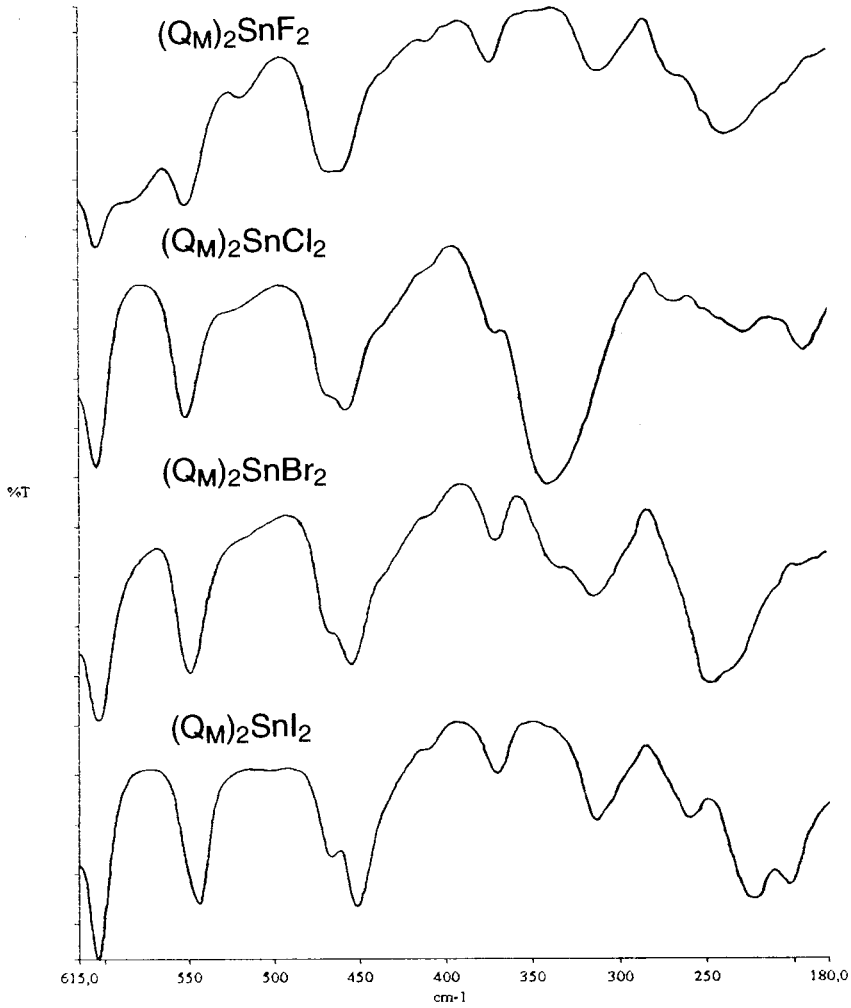

Fig. 3. Far-IR spectra of $(Q_M)_2SnX_2$.

$(Q)_2SnR_2$ derivatives. Carbon atoms C(3), C(4), C(5) and those of the R^2 and R^3 groups are deshielded and resonate upfield, whereas those of R^1 and of the chain carbonyl are downfield shifted upon coordination.

When at least one halogen is bonded to tin, several isomers are present in solution.

The $^nJ_{(Sn-H)}$ coupling constants are typical of trans six-coordinate tin compounds [15]. The $^1J_{(Sn-C)}$ of di-*n*-butyltin(IV) derivatives **2** and **9** and of diethyltin(IV) and dicyclohexyltin(IV) derivatives **1**, **4** and **11** can be used, in the empirical equations of Holecek [16] and of Lockhart [17] respectively, to derive C–Sn–C values (155 for **1**, 161 for **2**, 149 for **4**, 163 for **9** and 149° for **11**) which indicate distorted *trans* octahedral configurations.

The proton and carbon spectra of all the dihalotin(IV) derivatives always show two, three or four sets of resonances, due to the presence of isomers in solution.

We have carried out variable temperature ^{1}H-NMR experiments for the $(Q_D)_2SnF_2$ and $(Q_D)_2SnCl_2$ complexes in 1,1,2,2-tetrachloroethane-d_2 in the range 0–130°C (Fig. 4). The solvent was chosen because of its long liquid range and its homologous relationship with deuterated chloroform and dichloromethane. 1,1,2,2-Tetrachloroethane has a single sharp resonance at 2.17 ppm, which does not overlap with any of the derivative absorptions.

The methyl region between 2.20 and 3.60 ppm shows, at room temperature (r.t.), three main groups of bands, one for each methyl of the donor (Q_D) (N(1)–Me, C(3)–Me and (C=O)–Me). Each group is composed of two or four signals, with additional broadening and side bands caused by long-range (^{1}H–^{19}F) coupling in the spectrum of $(Q_D)_2SnF_2$. The increase of the temperature causes a progressive broadening and coalescence of the resonances. As expected, at 130°C only three distinct signals are present in the spectrum of $(Q_D)_2SnF_2$, thus indicating a fluxionality between the possible configurations on the NMR time-scale. Instead, for $(Q_D)_2SnCl_2$ at 135°C the coalescence is not complete, thus indicating a higher activation energy for the rearrangement in solution of the latter compound.

Table 3
^{1}H-NMR data (in $CDCl_3$) of compounds **1–26**

No.	Compound	R^2	R^1	R^3	Sn–R	Other data[a]
	Q_MH	2.02s	3.66s	7.40–7.63m		9.20–9.60sbr (O–H···O)
1	$(Q_M)_2SnEt_2$	1.78s	3.60s	7.45–7.52m	1.18t 1.60q	$^2J = 96.0,90.8$ $^3J = 160.4,153.1$
2	$(Q_M)_2SnBu^n_2$	1.75s	3.58s	7.40–7.52m	0.77t 1.25m 1.55m	
3	$(Q_M)_2SnBu^t_2$	1.75s	3.60s	7.38–7.60m	1.20s	$^3J = 134.8,126.1$
4	$(Q_M)_2SnCy_2$	1.75s	3.55s	7.40–7.52m	1.12m 1.45m 1.97m	
5	$(Q_M)_2SnBz_2$	1.75s	3.48s	7.30–7.55m	2.93s 6.95m	$^2J = 124.3,119.7$
6	$(Q_M)_2SnPh_2$	1.76sbr	3.52sbr	7.30–7.45m	7.50m 7.70m 8.12dd	
	Q_DH	2.38s	3.57s	2.41s		
7	$(Q_D)_2SnMe_2$	2.36s	3.50s	2.34s	0.74s	$^2J = 103.1,98.9$
8	$(Q_D)_2SnEt_2$	2.38s	3.51s	2.36s	1.08t 1.42q	$^2J = 95.8,91.7$ $^3J = 158.3,150.0$
9	$(Q_D)_2SnBu^n_2$	2.38s	3.49s	2.35s	0.78t 1.26m 1.42m	
10	$(Q_D)_2SnBu^t_2$	2.38s	3.50s	2.36s	1.11s	$^3J = 132.7,126.9$
11	$(Q_D)_2SnCy_2$	2.38s	3.48s 3.51s	2.36s 2.42s	1.15m 1.50m 1.85m	
12	$(Q_D)_2SnBz_2$	2.22s	3.38s	2.17s	2.73s	$^2J = 125.2,121.2$
13	$(Q_D)_2SnPh_2$	2.32s	3.40sbr	2.28sbr	7.35m 7.58d 7.62d	$^1J = 86.9$
14	$(Q_D)_2SnMeCl$	2.26s 2.32s	3.50s 3.55s	2.33s 2.50s 2.52s	0.92s 0.96s 1.04s	$^2J = 128.6,125.3$ 123.3,120.0
15	$(Q_D)_2SnCl_2$	2.40s 2.41s	3.45s 3.60s	2.44s 2.46s 2.60s		
16	$(Q_D)_2SnF_2$	2.40s[b] 2.42s[c]	3.48s[d] 3.60s[e]	2.46s 2.48s 2.59s 2.62s		
17	$(Q_D)_2SnBr_2$	2.42s 2.44s	3.43s 3.61s	2.47s 2.50s		
18	$(Q_D)_2SnI_2$	2.38s 2.40s 2.42s	3.40s 3.42s 3.58s	2.45s 2.47s 2.58s 2.62s		
19	$(Q_M)_2SnF_2$	 1.80s 1.87s 2.08s 2.12s	1.75s 3.50s 3.52s 3.62s 3.67s	3.40s 8.06dbr 3.70s	7.40–7.70mbr	
20	$(Q_M)_2SnBr_2$	1.78s 1.87s 1.90s 2.04s	3.45s 3.48s 3.58s 3.62s	7.40–7.70mbr 3.64s 3.68s		
21	$(Q_M)_2SnI_2$	1.78s 1.86s	2.44s 2.46s	7.38–7.66mbr		

Table 3 (continued)

No.	Compound	R^2	R^1	R^3	Sn–R	Other data[a]
		1.88s	2.62s			
		1.92s	2.67s			
22	$(Q')_2SnF_2$[f]	1.80s	7.20–7.40m	7.20–7.40m		
		1.82s	7.42–7.60m	7.42–7.60m		
		1.90s	7.62–7.75m	7.62–7.75m		
		2.00s	7.95d	7.95d		
23	$(Q')_2SnI_2$[f]	1.68s	7.15–7.40m	7.15–7.40m		
		1.78s	7.45–7.70m	7.45–7.70m		
		1.90s	7.95dd	7.95dd		
		2.02s				
24	$(Q'')_2SnF_2$[g]	2.17s, 2.48s		7.25–7.50m		
		2.51s, 2.53s		7.67t, 7.89dd		
		2.56s, 2.65s				
		2.68s, 2.70s				
25	$(Q'')_2SnBr_2$[g]	2.35s, 2.43s		7.15–7.40m		
		2.47s, 2.51s		7.48t, 7.67dd		
		2.53s, 2.60s		7.92dd		
		2.67s				
26	$(Q'')_2SnI_2$[g]	2.30s, 2.42s		7.16–7.42m		
		2.44s, 2.50s		7.50t, 7.64d		
		2.53s, 2.55s		7.95dd		
		2.58s, 2.65s				

[a] J in Hz.
[b] $J(H–F) = 2.2$ Hz.
[c] $J(H–F) = 4.0$ Hz.
[d] $J(H–F) = 7.7$ Hz.
[e] $J(H–F) = 5.5$ Hz.
[f] Signals of R^1 and R^3 are indistinguishable.
[g] Signals of R^1 and R^2 are indistinguishable.

In the same solvent comparable coalescence temperatures and two bands were shown by analogous acetylacetonate derivatives; these exist in solution as two *cis* isomers ([14]b). Instead, our derivatives are likely to exist in solution as a mixture of *cis* and *trans* isomers, as indicated by the presence of more than two sets of signals.

There are reports in the literature on possible mechanisms for configurational rearrangements of dihalobis(β-diketonate)tin(IV) complexes ([14]b)[18]. These include:

1. complete dissociation of one β-diketonate donor, to give a four- coordinate intermediate;
2. dissociation of a halide ion, to give a five-coordinate intermediate;
3. breaking of one M–O bond also to give, in this case, a five-coordinate intermediate, with a monodentate β-diketonate donor;
4. twisting mechanisms and consequent rearrangement without any metal–ligand bond breaking.

Intermolecular mechanisms (1) and (2) are improbable based on evidence from acetylacetonatetin(IV) derivatives ([14]b), and our complexes. In fact, it is possible from the lack of conductivity in dichloromethane solution, to exclude both the following dissociative equilibria:

$$(Q)_2SnX_2 \rightleftharpoons [(Q)SnX_2]^+ + Q^-$$

$$(Q)_2SnX_2 \rightleftharpoons [(Q)_2SnX]^+ + X^-$$

Although we cannot indicate which of the intramolecular mechanisms (3) or (4) could be operating in the present study, difficulty in obtaining crystals useful for diffraction study of bis(β-diketonate)dihalotin(IV) derivatives may be ascribed to a mixture of isomers and fluxionality.

^{19}F-NMR spectra also have been carried out for $(Q)_2SnF_2$ derivatives (Table 5). They show one or two absorptions in the range between $+160$ and $+186$ ppm relative to the external $CFCl_3$ standard. They are deshielded with respect to $(acac)_2SnF_2$ ($+153$ ppm) ([14]b), thus indicating that fluorine atoms behave more as donating ligands in our derivatives. Moreover, the deshielding increases on going from $(Q_D)_2SnF_2$ ($+160$ ppm) to $(Q')_2SnF_2$ ($+186$ ppm), in accord with a decrease of the $(Q)^-$ donor power, caused by a progressive substitution of one and two Me with Ph groups in R^1 and R^3 positions of the acylpyrazolonates. This trend can be explained in terms of the Pauling Electroneutrality Principle: the more electron donating are the β-diketonate ligands, the less electron donating are the fluorine atoms, and vice versa.

Table 4
^{13}C-NMR data (in $CDCl_3$) of compounds **1–15**, **23**, **25** and **26**

No.	Compound	R^2	R^1	R^3	CO C(5)	C(3) C(4)	R–Sn	Other data[a]
	Q_MH	15.5	32.5	127.7,128.3 130.0,138.4	193.0 160.4	147.0 102.3		
1	$(Q_M)_2SnEt_2$	16.3	31.8	127.4,128.2 130.8,139.8	191.4 162.7	148.1 103.5	9.4 21.7	$^1J = 891.7,851.9$
2	$(Q_M)_2SnBu^n_2$	16.8	32.2	127.9,128.8 131.3,140.4	191.8 163.2	148.5 104.0	14.1,26.4 27.5,29.1	$^1J = 860.5,822.7$ $^2J = 44.4$ $^3J = 129.5$
3	$(Q_M)_2SnBu^t_2$	16.4	31.6	127.4,128.2 130.7,140.1	n.o. n.o.	147.7 n.o.	29.2 50.3	
4	$(Q_M)_2SnCy_2$	16.8	32.2	127.8,128.8 131.1,140.7	192.0 163.3	148.5 104.3	27.4,29.0 29.3,30.0 30.3,47.6	$^1J = 819.1,785.7$ $^2J = 20.5$ $^3J = 94.7$
5	$(Q_M)_2SnBz_2$	16.5	32.2	127.6,128.6 131.5,138.6	n.o.	148.4 104.2	36.8,124.6 127.8,129.5 139.8	$^3J = 51.2$ $^4J = 32.6$
6	$(Q_M)_2SnPh_2$	15.8	32.1	127.9,128.7 131.2,138.5	190.3br 163.9br	148.0 103.8	128.3,128.7 135.2, n.o.	$^2J = 58.8$ $^3J = 86.9$ $^4J = 19.7$
	Q_DH	15.3	32.3	27.2	195.0 159.4	146.6 103.0		
7	$(Q_D)_2SnMe_2$	17.1	31.7	27.7	192.2 161.8	147.7 103.6	8.2	
8	$(Q_D)_2SnEt_2$	17.1	31.6	27.6	192.7 161.8	147.5 103.7	9.3 21.2	
9	$(Q_D)_2SnBu^n_2$	17.6	32.1	28.1	193.1 162.2	147.9 104.1	14.1,26.4 27.3,28.5	$^1J = 880.0,841.4$ $^2J = 43.5$ $^3J = 129.6$
10	$(Q_D)_2SnBu^t_2$	17.1	31.4	27.8	193.3 n.o.	147.2 104.7	29.1 49.5	
11	$(Q_D)_2SnCy_2$	17.2	31.5	27.6	192.7 161.9	147.1 104.0	26.5,26.8 28.5,28.8 29.6,30.0	$^1J = 820.0,800.0$ $^2J = 23.1$ $^3J = 90.4$
12	$(Q_D)_2SnBz_2$	17.4	31.9	27.6	193.1 n.o.	148.0 104.2	36.4,124.5 127.8,129.5 140.1	$^3J = 50.5$ $^4J = 30.5$
13	$(Q_D)_2SnPh_2$	17.5	32.1	27.5	n.o. n.o.	148.9 n.o.	128.5,129.1 135.6,148.4	$^2J = 59.6,56.0$ $^3J = 93.0,89.2$ $^4J = 19.0$
14	$(Q_D)_2SnMeCl$	16.8 17.0	31.8 32.1	26.6 26.6 26.8 26.5	192.0 192.6 162.4	148.4 104.1 104.3	9.9 10.2 11.7	
15	$(Q_D)_2SnCl_2$	17.1 17.2	27.4 27.6	21.8 21.9 22.0 22.5	188.5 188.8 189.2 159.0 159.2	144.6 144.6 99.8 100.1		
23	$(Q')_2SnI^b_2$	16.2 16.3 16.4 16.5	120.9,121.2,121.6 121.7,126.7,126.9 127.1,127.2,128.3 128.4,128.5,128.6 128.7,128.8,128.9 129.0,129.1,132.3 132.5,132.7,136.7 136.8,136.9		190.0 190.1 190.4 162.1 162.3 162.4	150.0 150.1 150.3 n.o.		
25	$(Q'')_2SnBr_2$	16.9 17.0 17.1 17.2	121.0 121.6 121.7 126.9 127.0 127.1 127.2	27.0 27.1 27.2 27.3	193.9 194.2 194.7 161.2 161.9 162.0	149.9 150.0 150.3 105.2 105.4 105.5		

Table 4 (continued)

No.	Compound	R^2	R^1	R^3	CO C(5)	C(3) C(4)	R–Sn	Other data[a]
			128.5					
			128.9					
			129.0					
			129.1					
			136.7					
			136.8					
			136.9					
26	$(Q'')_2SnI_2$	16.9	120.9	26.9	192.9	150.0		
		17.0	121.5	27.1	193.4	150.3		
		17.1	121.6	27.3	194.2	104.8		
			126.8		161.5	105.0		
			126.9		161.8			
			127.0					
			128.7					
			128.9					
			129.0					
			129.1					
			136.7					
			136.9					

[a] J in Hz.
[b] Signals of R^1 and R^3 are indistinguishable.

The ^{119}Sn-NMR data support our previous conclusions. In the spectra of **1–13** there is only one resonance. The values of $\delta(^{119}Sn)$ observed are in agreement with the trends reported in the literature [15]. They are a function of the nature of R groups linked to tin and decrease in the following order:

$$Me < Bu^n < Et < Cy < Bu^t < Bz < Ph$$

The effect caused by the substitution of each Me group by a chlorine atom is roughly additive. In Fig. 5 the trend of $(Q_D)^-$ derivatives **7**, **14** and **15** is compared with that of the $(Q_M)^-$ analogues previously synthesized ([6]a). It seems that the ligand $(Q_D)^-$ behaves as a better donor than $(Q_M)^-$, due to the presence of three electron releasing methyls in R^1, R^2 and R^3 positions, which increase the 'σ' donor character.

In Fig. 6 the effect of increasing substitution in R groups bonded to tin on the ^{119}Sn chemical shift can be seen. As expected, such an increase leads to a higher donor character of the alkyl groups ($Me < Et < Cy < Bu^t$) and is the reason for the electron density increase on the tin atom.

This is the first ^{119}Sn-NMR report for derivatives having a SnO_4X_2 core, where X stands for the complete series of the halogens F, Cl, Br and I. In the literature, some reports ([14]b)([18]a) dealing with IR and ^{1}H-NMR trends for dihalotin(IV)(O_2-donor)$_2$ exist.

The $(Q)_2SnF_2$ derivatives absorb in the range from -740– -770 ppm relative to $SnMe_4$, giving rise to two main groups of signals stemming from (^{119}Sn–^{19}F) coupling. These are of the order of 2050/2250 Hz, relatively higher than those observed in $(acac)_2SnF_2$, (1850/1950 Hz) ([14]b), and in accord with the previously discussed stronger Sn–F linkage in our derivatives.

The $(Q)_2SnCl_2$ resonances fall between -620 and -650 ppm, those of $(Q)_2SnBr_2$ between -850 and -880 ppm and finally the $(Q)_2SnI_2$ derivatives absorb from -1300– -1470 ppm. The latter are the most ^{119}Sn shielded bis(acylpyrazolonate)tin(IV) derivatives synthesized. However in the literature, other SnO_4I_2 complexes are known to absorb at more negative fields, for example bis(tetraphenylimidodiphosphinato) diiodotin(IV) shows a signal at -1759 ppm [19]. In Fig. 7 the trend of ^{119}Sn chemical shifts as a function of the type of halogens bonded to tin is reported: on going from F to I the absorptions describe a 2nd order polynomial function, similar to those reported in the case of R_nSnCl_{4-n} [20].

This feature can be explained by the electron withdrawing inductive effect of the halogens and, also, by a possible additional π contribution to the Sn–X bonds [20,21], in the case of Cl, Br and I, which would shield the tin nucleus to a greater extent. This *trans*-inductive effect can be schematically indicated:

$$O - Sn - \vec{X} \text{ (where X = Cl, Br and I)}$$

It is probable that in the case of difluorotin(IV) derivatives, whose resonances fall in the range between those of $(Q)_2SnCl_2$ and $(Q)_2SnBr_2$, the reverse effect is operating.

$$O - Sn - \vec{F}$$

This is due to the higher electronegativity of fluorine compared to oxygen and the lack of π contribution to the Sn–F bond.

2.4. Diffraction study of $(Q_D)_2SnCy_2$ (12)

The crystal structure of the title compound, $(Q_D)_2SnCy_2$, is composed of well separated and discrete molecules as there are no intermolecular contacts shorter than the van der Waals radii of the atoms. Atomic coordinates for non-H atoms are given in Table 6; those for H atoms are in the supplementary material.

Table 5
^{119}Sn and ^{19}F-NMR data[a] ($CDCl_3$) of derivatives **1–26**

Compound	No.	$\delta(^{119}Sn)$	Other data	$\delta(^{19}F)$
$(Q_M)_2SnEt_2$	**1**	−349.9		
$(Q_M)_2SnBu^n_2$	**2**	−345.5		
$(Q_M)_2SnBu^t_2$	**3**	−448.5		
$(Q_M)_2SnCy_2$	**4**	−421.3		
$(Q_M)_2SnBz_2$	**5**	−449.0		
$(Q_M)_2SnPh_2$	**6**	−485.1		
$(Q_D)_2SnMe_2$	**7**	−312.9		
$(Q_D)_2SnEt_2$	**8**	−351.6		
$(Q_D)_2SnBu^n_2$	**9**	−347.2		
$(Q_D)_2SnBu^t_2$	**10**	−448.5		
$(Q_D)_2SnCy_2$	**11**	−427.7		
$(Q_D)_2SnBz_2$	**12**	−449.9		
$(Q_D)_2SnPh_2$	**13**	−490.3		
$(Q_D)_2SnMeCl$	**14**	−492.6, −493.0		
		−495.4, −499.4		
$(Q_D)_2SnCl_2$	**15**	−629.4, −632.9		
		−637.0		
$(Q_D)_2SnF_2$	**16**	−751.1	$^1J(Sn–F)$ = n.o.	+160.2
		−770.4	$^1J(Sn–F)$ = n.o.	
$(Q_D)_2SnBr_2$	**17**	−849.4, −861.4		
		−872.8		
$(Q_D)_2SnI_2$	**18**	−1318.2,		
		−1371.9		
		−1441.4,		
		−1477.3		
$(Q_M)_2SnF_2$	**19**	−743.7	$^1J(^{119}Sn–^{19}F) = 2234.0$	+185.1
			$^1J(^{117}Sn–^{19}F) = 2188.1$	
		−752.5	$^1J(^{119}Sn–^{19}F) = 2297.9$	
			$^1J(^{117}Sn–^{19}F) = 2160.6$	
$(Q_M)_2SnBr_2$	**20**	−731.4, −735.6		
		−739.9, −744.4		
		−848.0, −858.5		
		−867.2, −868.9		
$(Q_M)_2SnI_2$	**21**	−1318.2,		
		−1371.9		
$(Q')_2SnF_2$	**22**	−749.4	$^1J(^{119}Sn–^{19}F) = 2200.4$	+184.7
			$^1J(^{117}Sn–^{19}F) = 2131.7$	+186.4
		−758.0	$^1J(^{119}Sn–^{19}F) = 2237.0$	
			$^1J(^{117}Sn–^{19}F) = 2179.1$	
$(Q')_2SnI_2$	**23**	n.o.[b]		
$(Q'')_2SnF_2$	**24**	−745.7	$^1J(^{119}Sn–^{19}F) = 2255.3$	+176.5
			$^1J(^{117}Sn–^{19}F) = 2074.6$	
		−755.6	$^1J(^{119}Sn–^{19}F) = 2215.6$	
			$^1J(^{117}Sn–^{19}F) = 2179.1$	
$(Q'')_2SnBr_2$	**25**	−859.3, −869.6		
		−879.2		
$(Q'')_2SnI_2$	**26**	n.o.[b]		

[a] In ppm from external standard $Sn(CH_3)_4$ and $CFCl_3$, respectively.
[b] Probably due to low solubility of compound in $CDCl_3$.

Selected bond distances and angles are given in Table 7 and an ORTEP view of the molecule, with H atoms omitted for clarity, is shown in Fig. 8.

The molecular structure of the title compound shows the tin having coordination number six and the metal octahedral geometry strongly distorted as shown in previous related complexes. The coordination polyhedron is formed by four O atoms, from two chelating pyrazolonates, and two C atoms, from the cyclohexyl groups. The four O atoms lie in the equatorial plane and the four O–Sn–O *cis* bond angles equal 360°.

The organic groups are trans to each other although a strong distortion from 180° is found and the angle is 154.6(5)°. Another common feature in these complexes is two different sets of Sn–O distances. Thus, for one ligand there is a short bond length Sn–O1 = 2.094(9) Å (primary bond) and a longer one, Sn–O2 = 2.42(1) Å (secondary bond). For the other ligand the corresponding values are Sn–O51 = 2.132(9) Å and Sn–O52 = 2.405(8) Å. This asymmetry in bond length is a result of asymmetric nature of the ligand.

In contrast, a symmetric ligand (acacH) stabilizes the perfect octahedral complex $(acac)_2Sn(CH_3)_2$ ([5]a) with the metal on an inversion center and the same coordination environment as the title compound. In addition, the equatorial plane made by the four O atoms has the oxygen atoms associated with the primary bonds, O1 and O51, closer to each other than those associated with the secondary bonds, O2 and O52, as shown by the corresponding angles O1–Sn–O51 = 77.8(3)° and O2–Sn–O52 = 121.2(3)°.

The location of the cyclohexyl groups relative to the equatorial plane is such that they are folded towards the side of the secondary bonds. This feature decreases the repulsion among the corresponding atoms in the coordination sphere. The cyclohexyl groups show C10 and C16 displayed symmetrically above and below the equatorial plane (the angle between the bond Sn–C10 and the equatorial plane is 77° and that between the bond Sn–C16 and the equatorial plane is 78°). The title compound structure has approximate C_s symmetry.

In previous related structures [1,6,22], a phenyl group is the substituent on N1. This Ph group is coplanar with the attached pyrazole ring and has an intramolecular separation between an *ortho*-H atom and O1 of about 2.2 Å; such a distance is shorter than the corresponding sum of the van der Waals parameters (1.20 Å (H) + 1.40 Å (O) = 2.60 Å [23]). Instead, the title compound has a methyl group (C6) rather than a Ph group. This methyl has a H at a longer distance from O1, greater than 2.48 Å according to a model scheme (see Section 3). This implies that the C–O···H interactions are certainly weaker in this complex than those found in previous structures. Nevertheless, the distortion in this complex is of the same order as found for the other

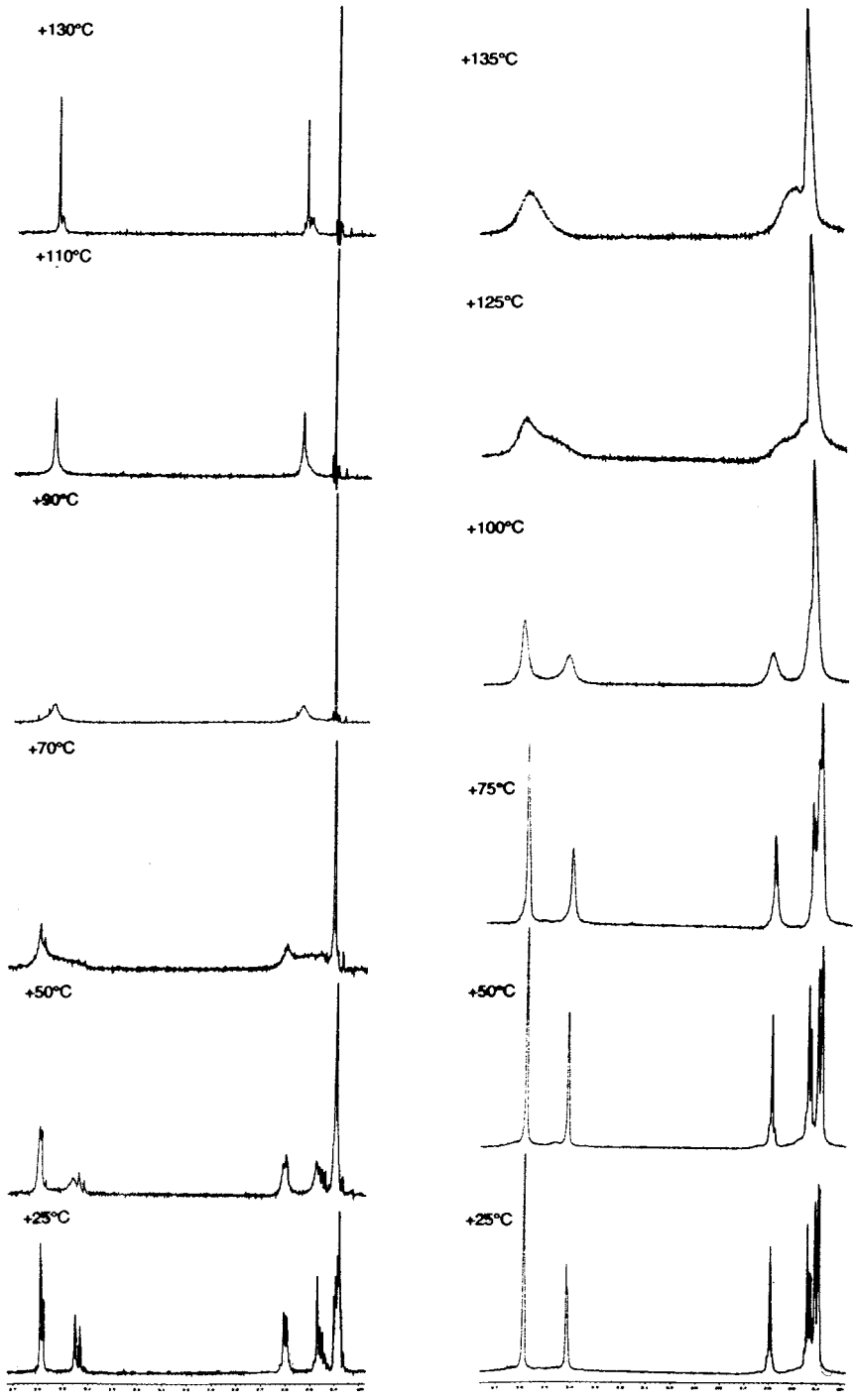

Fig. 4. ^{1}H-NMR variable temperature experiments of $(Q_D)_2SnF_2$ (a) and of $(Q_D)_2SnCl_2$ (b).

dialkyltins pyrazolonates (range 150–162°), thus the characteristic distortion (skewed trapezoidal bipyramidal, STB) of this family of complexes cannot be ascribed solely to the C–O···H interaction.

Selected structural parameters for related species are shown in Table 8 and, for comparison purposes, this Table includes $(acac)_2Sn(CH_3)_2$ as well. Some parameters in Table 8 show clear trends. Thus, increasing the C–Sn–C angle is associated with:

1. a smaller difference in bond length between primary and secondary bonds (Sn–O1 and Sn–O2);
2. a smaller difference between O_s–Sn–O_s and O_p–Sn–O_p (O_s/O_p = oxygen atom associated to secondary/primary bond);

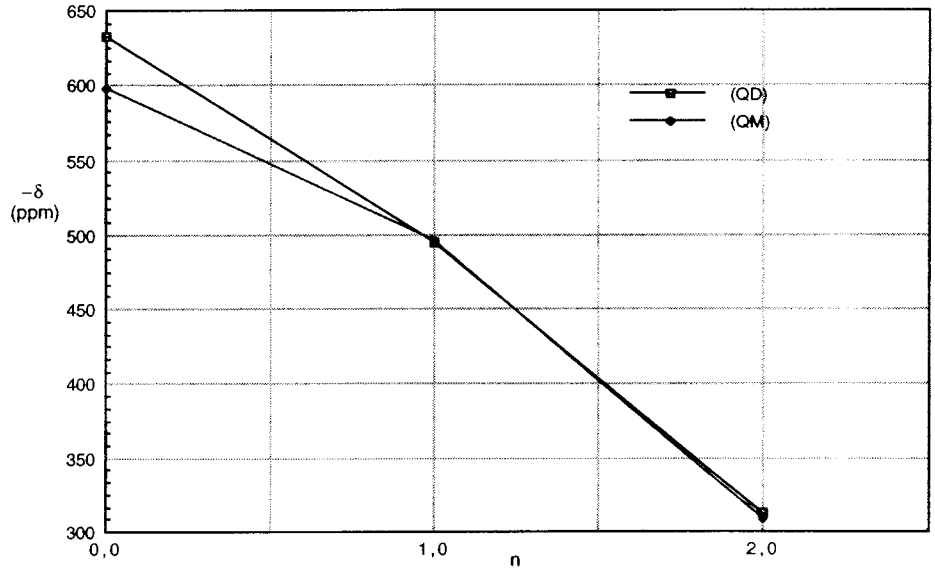

Fig. 5. Substituent effect on the ^{119}Sn chemical shift of $(Q)_2Me_nSnCl_{2-n}$ ($Q = Q_D$ and Q_M, average value for $n = 0$ and $n = 1$).

3. an increasing bite angle O1–Sn–O2 (and O51–Sn–O52 in the other ligand);
4. less deformation of the octahedron.

The bite angle is considered a principal reason for the octahedral deformation by Kepert [7] who calculated the repulsion among the atoms forming the coordination sphere and defined the distorted system as STB. From results of energy calculations on STB complexes containing symmetric ligands, Kepert concluded that the smaller the bite angle, the stronger the distortion. Table 8 shows that the same conclusion holds for asymmetric ligands.

The structural behavior of these complexes can be explained on the basis of the chemical modifications:

1. the organic groups attached to the metal;
2. the ligand substituent on C8;
3. the ligand substituent on N1.

In the first case, as shown ([6]c) previously, the phenyl groups attached to the tin atom stabilize the largest C–Sn–C bond angle (173.0°). The electronic nature (withdrawing effect) of this group is considered responsible for this value ([6]c). On the contrary, alkyl groups attached to the metal (better electron donors than phenyl groups) show much smaller C–Sn–C angles (about 150–162°). It is observed that the distortion induced by the cyclohexyl group, which is a tertiary alkyl group, in the title compound is of the same order as that found for alkyl groups. Moreover, a comparison of the effect of a primary methyl group in $(Q')_2Sn(Me)_2$ (C–Sn–C = 153.3(3)°) ([6]a), that of a secondary *n*-butyl group in $(Q')_2Sn(Bu^n)_2$ (C–Sn–C = 154.7(8)°) ([22]a) and that of a quaternary *t*-butyl group in $(Q')_2Sn(Bu^t)_2$ (C–Sn–C = 150.0(5)°) [1] shows even more similarity in the octahedral distortion with the title compound which has a C–Sn–C of 154.6(5)°. Therefore, the structural behavior of the title compound appears to corroborate previous results. This comparison does not take into account the differences among ligands (Q′ and Q_D) and such an assumption appears reasonable as shown below.

With respect to the second modification, substitution on C8, it is apparent that this change implies less structural variation on the whole complex than that obtained by substitution on the metal. However, there are not yet sufficient complexes studied to elucidate the rules governing such structural variations. The same applies for substitution on N1. We will further investigate this point.

3. Experimental section

3.1. General comments

The tin(IV) and organotin(IV) halides were purchased from Alfa (Karlsruhe) and Aldrich (Milwaukee) and used as received, except for dibenzyltin dichloride which was synthesized according to a reported procedure [24].

The samples for microanalysis were dried in vacuo to constant weight (20°C, ca. 0.1 Torr). Elemental analyses (C, H, N) were performed in house with Fisons Instruments 1108 CHNS-O Elemental analyzer. Molecular weight determinations were performed with a Knauer membrane osmometer. IR spectra were recorded from 4000–100 cm^{-1} with a Perkin-Elmer System 2000 FT-IR instrument. ^{1}H, ^{13}C, ^{19}F and ^{119}Sn-NMR spectra were recorded on a VXR-300 Varian spectrometer operating at r.t. (300 MHz for ^{1}H, 75 MHz for ^{13}C, 282.2 MHz for ^{19}F and 111.9 MHz for

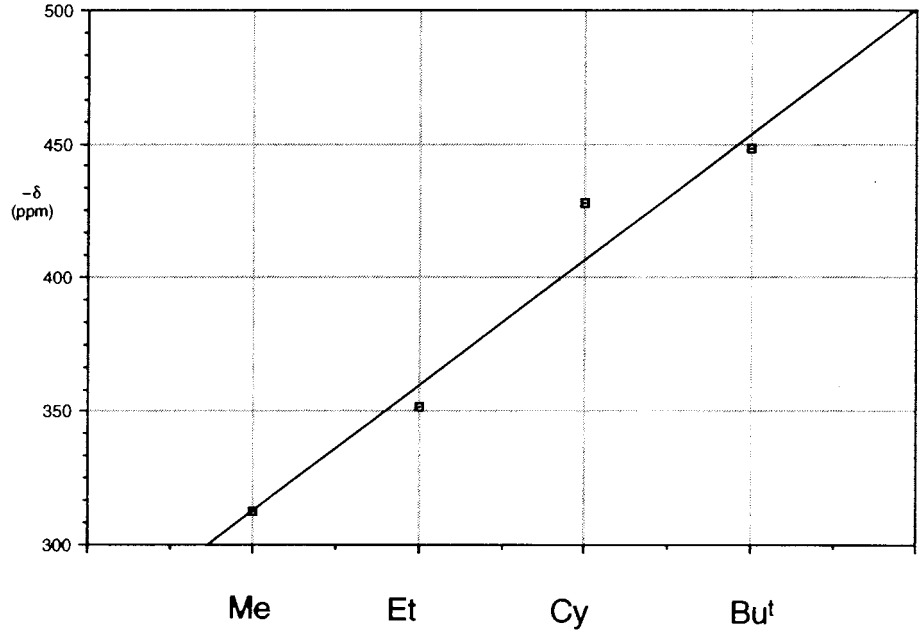

Fig. 6. The effect of increasing substitution of R on the ^{119}Sn chemical shift of $(Q_D)_2SnR_2$ (R = Me, Et, Cy, Bu^t).

^{119}Sn). Melting points were taken on an IA 8100 Electrothermal instrument. The electrical conductance of the dichloromethane solutions was measured with a Crison CDTM 522 conductimeter at r.t.

3.2. Synthesis of the donors

The precursor 1,3-dimethyl-5-pyrazolone was synthesized by a reported procedure [25].

3.2.1. Synthesis of Q_MH

1,3-Dimethyl-5-pyrazolone (6.0 g, 53.5 mmol) was placed in a flask equipped with a stirrer, separating funnel and a reflux condenser and dissolved in dry dioxane (60 ml) by warming. Calcium hydroxide (10.0 g, 135 mmol) and then benzoyl chloride (6.5 ml, 7.9 g, 56.0 mmol) were added, the latter dropwise for 10 min. The mixture was heated to reflux overnight and then poured into HCl 2 N (200 ml) to decompose the calcium complex. The resulting clear solution was heated to reduce the volume to one half, then ice was added and a precipitate formed. It was filtered and recrystallized from methanol–water and dried to constant weight (8.2 g, 38.2 mmol, 71% yield).

3.2.2. Synthesis of Q_DH

1,3-Dimethyl-5-pyrazolone (6.0 g, 53.5 mmol) was placed in a flask equipped with a stirrer, separating funnel and a reflux condenser and dissolved in dry dioxane (60 ml) by warming. Calcium hydroxide (10.0 g, 135 mmol) and then acetyl chloride (3.8 ml, 4.2 g, 54.0 mmol) were added, the latter dropwise for 10 min. The mixture was heated to reflux overnight and then poured into HCl 2 N (200 ml) to decompose the calcium complex. The resulting clear solution was heated to reduce the volume to one half, then dichloromethane (100 ml) was added and two phases formed. The organic phase, separated from the aqueous phase, was evaporated under reduced pressure to give a light brown solid, which was recrystallized from diethyl ether and dried to constant weight (4.6 g, 29.4 mmol, 55% yield).

3.3. Synthesis of the complexes

3.3.1. Diethyltin(IV)bis(1,3-dimethyl-4-benzoylpyrazolon-5-ato) $(Q_M)_2SnEt_2$ (1)

Diethyltin dichloride (0.248 g, 1 mmol) was added to a methanolic solution (30 ml) of the ligand Q_MH (0.432 g, 2 mmol) and KOH (0.112 g, 2 mmol). The clear solution was stirred overnight at r.t., then water was added (15 ml). Immediately a precipitate formed, which was filtered, recrystallized from a mixture of chloroform and light petroleum and dried to constant weight. The complexes $(Q_D)_2SnMe_2$, $(Q_D)_2SnEt_2$ and $(Q_D)_2SnMeCl$ were synthesized by the same procedure.

3.3.2. Di-n-butyltin(IV)bis(1,3-dimethyl-4-benzoylpyrazolon-5-ato) $(Q_M)_2SnBu^n_2$ (2)

A benzene solution (20 ml) of di-*n*-butyltin oxide (0.248 g, 1 mmol) was added to a benzene solution (20 ml) of the ligand Q_MH (0.432 g, 2 mmol), and the reaction mixture was refluxed for about 6 h. After removing the solvent under reduced pressure on a rotary evaporator, a thick oil was obtained. This was dissolved in diethyl ether (40 ml) and the solution left

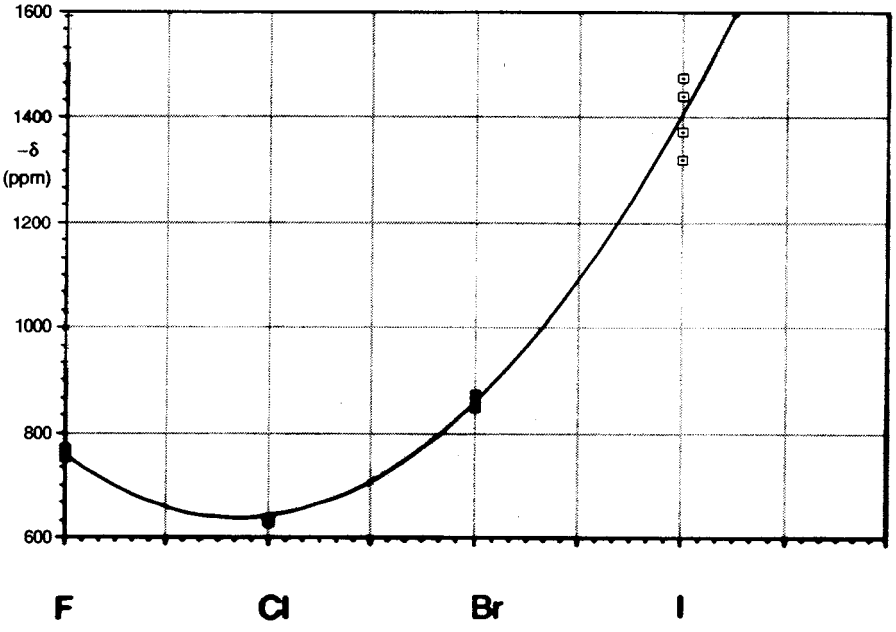

Fig. 7. Halogen effect on ^{119}Sn chemical shift of $(Q_D)_2SnX_2$ (X = F, Cl, Br and I).

to evaporate until a yellow precipitate formed. This was filtered, recrystallized from methanol/diethyl ether and dried to constant weight. The complex $(Q_D)_2SnBu^n_2$ was obtained using the same procedure.

3.3.3. Di-t-butyltin(IV)bis(1,3-dimethyl-4-benzoylpyrazolon-5-ato) $(Q_M)_2SnBu^t_2$ (3)

Di-*t*-butyltin dichloride (0.304 g, 1 mmol) was added to a methanolic solution (30 ml) of the ligand Q_MH (0.432 g, 2 mmol) and KOH (0.112 g, 2 mmol). The clear solution was stirred overnight at room temperature, then evaporated to dryness under reduced pressure on a rotary evaporator. The residue was treated with chloroform (20 ml) and to the filtered solution diethyl ether was added (40 ml): a yellow precipitate formed, which was filtered, recrystallized from diethyl ether and dried to constant weight. The complex $(Q_D)_2SnBu^t_2$ was obtained using the same procedure but light petroleum was used instead of diethyl ether.

3.3.4. Dicyclohexyltin(IV)bis(1,3-dimethyl-4-benzoylpyrazolon-5-ato) $(Q_M)_2SnCy_2$ (4)

Dicyclohexyltin dibromide (0.445 g, 1 mmol) was added to a methanolic solution (30 ml) of the ligand Q_MH (0.432 g, 2 mmol) and KOH (0.112 g, 2 mmol). The clear solution was stirred overnight at r.t., then evaporated to dryness under reduced pressure on a rotary evaporator. The residue was treated with chloroform (20 ml) and to the filtered solution diethyl ether was added (40 ml). From the solution, left to evaporate overnight at r.t., a light brown precipitate formed, which was filtered, recrystallized from a mixture of methanol/diethyl ether and dried to constant weight. The complexes $(Q_D)_2SnCy_2$, $(Q_D)_2SnCl_2$, $(Q_D)_2SnBr_2$ and $(Q_M)_2SnBr_2$ were synthesized using the same procedure.

3.3.5. Dibenzyltin(IV)bis(1,3-dimethyl-4-benzoylpyrazolon-5-ato) $(Q_M)_2SnBz_2$ (5)

Dibenzyltin dichloride (0.372 g, 1 mmol) was added to a methanolic solution (30 ml) of the ligand Q_MH (0.432 g, 2 mmol) and KOH (0.112 g, 2 mmol). The clear solution was stirred overnight at r.t., then evaporated to dryness under reduced pressure on a rotary evaporator. The residue was treated with dichloromethane (20 ml) and methanol was added (40 ml) to the filtered solution. A precipitate formed, which was filtered, recrystallized from ethyl acetate and dried to constant weight. The complexes $(Q_M)_2SnPh_2$, $(Q_D)_2SnBz_2$ and $(Q_D)_2SnPh_2$ were synthesized using the same procedure.

3.3.6. Difluorotin(IV)bis(1,3-dimethyl-4-acetylpyrazolon-5-ato) $(Q_D)_2SnF_2$ (16)

Tin tetrafluoride (0.195 g, 1 mmol) was added to a dichloromethane solution (40 ml) of the ligand Q_DH (0.312 g, 2 mmol). The resulting suspension was left to reflux with stirring for 2 days, then unreacted SnF_4 was removed by filtration of the hot solution and the filtrate was evaporated to dryness under reduced pressure on a rotary evaporator. The residue was extracted using hot diethyl ether (30 ml) from which a yellow precipitate slowly formed on cooling. The complexes $(Q_M)_2SnF_2$, $(Q')_2SnF_2$ and $(Q'')_2SnF_2$ were obtained in a similar way by using choloroform instead of dicholoromethane.

3.3.7. Diiodotin(iv)bis(1,3-dimethyl-4-acetyllpyrazolon-5-ato) $(Q_D)_2SnI_2$ (16)

To a THF solution (40 ml) of the derivative $(Q_D)_2SnCl_2$, (0.607 g, 1 mmol) was added an excess of NaI (0.600 g, 4 mmol) and the resulting suspension was left to reflux with stirring for 3 days. Then it was filtered to separate the excess NaI and the NaCl formed by the Cl/I exchange, and the filtrate was evaporated to dryness under reduced pressure on a rotary evaporator. The residue was recrystallized with methanol/diethyl ether. The complexes $(Q_M)_2SnI_2$, $(Q')_2SnI_2$ and $(Q'')_2SnI_2$ were synthesized in the same way.

3.4. X-ray diffraction

A preliminary study was performed using a Weissenberg Camera to determine cell parameters and space group. A $P2_1$ Syntex diffractometer was used for the measurements of the cell constants and for the data collection. A summary of crystal data together with details of data collection and computer resolution is given in Table 9. Monitoring of the standard reflections [0,4,0], [0, −4,0] and [1,1, −1], taken every 100 reflections, indicated no decay. A ψ-scan showed no absorption anisotropy. Data were corrected for Lorentz and polarization effects. The molecular structure was solved using the heavy atom method with CAOS [26]. Subsequent calculations were performed as follows: refinement based on the minimization of the function $\Sigma w(|F_o| - |F_c|)^2$ with the weighting scheme $w = 1/(a + F_o + cF_o^2)$, where a and c are of the order of $2F_o$(min) and $2/F_o$(max) [27], respectively; H atoms were introduced at fixed positions according to C–H distance = 0.96 Å. Anisotropic displacement parameters were allowed for non-H atoms and H isotropic displacement parameters were kept fixed during refinement. The final refinement showed no residual peaks. Atomic scattering factors and anomalous dispersion terms were taken from the literature [28].

Table 6
Atomic coordinates and isotropic displacement parameters

Sn	0.12540(2)	0.27023(4)	0.3089(1)	2.79(2)
O1	0.1350(3)	0.1674(5)	0.408(1)	3.7(2)
O2	0.0699(3)	0.2045(5)	0.183(1)	4.0(2)
O51	0.1780(2)	0.2880(4)	0.4552(9)	3.3(2)
O52	0.1364(3)	0.3972(5)	0.257(1)	3.8(2)
N1	0.1319(3)	0.0434(6)	0.437(1)	4.0(3)
N2	0.1115(4)	−0.0182(6)	0.381(1)	4.7(4)
N51	0.2248(3)	0.3518(7)	0.599(1)	4.4(3)
N52	0.2389(4)	0.4237(8)	0.626(1)	5.0(4)
C3	0.0839(4)	0.0074(7)	0.278(2)	3.8(4)
C4	0.0862(4)	0.0853(6)	0.265(1)	2.8(3)
C5	0.1177(4)	0.1062(6)	0.371(1)	3.1(3)
C6	0.1650(5)	0.0366(9)	0.551(2)	5.0(5)
C7	0.0578(5)	−0.0483(8)	0.192(2)	4.9(4)
C8	0.0638(4)	0.1358(7)	0.177(1)	3.3(3)
C9	0.0287(4)	0.114(1)	0.067(2)	5.8(5)
C10	0.1513(4)	0.2555(6)	0.110(1)	2.9(3)
C11	0.1608(4)	0.1752(6)	0.081(1)	3.1(3)
C12	0.1808(4)	0.1693(7)	−0.056(1)	3.9(4)
C13	0.1556(5)	0.2046(9)	−0.186(2)	4.9(4)
C14	0.1466(4)	0.2844(7)	−0.156(1)	4.1(4)
C15	0.1265(5)	0.2914(7)	−0.020(1)	4.3(4)
C16	0.0844(4)	0.3155(8)	0.439(2)	3.8(4)
C17	0.0535(4)	0.3654(9)	0.352(2)	5.2(5)
C18	0.0281(5)	0.400(1)	0.461(2)	6.9(6)
C19	0.0084(6)	0.342(1)	0.543(2)	7.4(7)
C20	0.0391(6)	0.291(1)	0.627(2)	7.2(7)
C21	0.0656(5)	0.258(1)	0.523(2)	5.8(5)
C53	0.2161(5)	0.4648(8)	0.536(2)	5.0(5)
C54	0.1863(4)	0.4257(8)	0.447(2)	4.5(4)
C55	0.1942(4)	0.3510(8)	0.493(1)	3.8(4)
C56	0.2445(4)	0.2905(8)	0.679(2)	4.9(4)
C57	0.2251(6)	0.547(1)	0.542(2)	7.6(7)
C58	0.1568(4)	0.4444(7)	0.330(2)	4.0(4)
C59	0.1494(6)	0.5237(8)	0.295(2)	6.2(6)

Table 7
Selected bond distances and angles

Distances	
Sn1–O1	2.094(9)
Sn1–O2	2.42(1)
Sn1–O51	2.132(9)
Sn1–O52	2.405(8)
Sn1–C10	2.17(1)
Sn1–C16	2.14(1)
O1–C5	1.29(1)
O2–C8	1.27(2)
O51–C55	1.30(2)
O52–C58	1.25(2)
Angles	
C(16)–Sn(1)–C(10)	154.6(5)
O(2)–Sn(1)–O(1)	80.4(3)
O(52)–Sn(1)–O(51)	80.5(3)
O(51)–Sn(1)–O(1)	77.8(3)
O(52)–Sn(1)–O(2)	121.2(3)
O(51)–Sn(1)–O(2)	158.2(3)
O(52)–Sn(1)–O(1)	158.3(4)
C(10)–Sn(1)–O(1)	101.6(4)
C(10)–Sn(1)–O(2)	85.3(4)
C(10)–Sn(1)–O(51)	98.4(4)
C(10)–Sn(1)–O(52)	81.8(4)
C(16)–Sn(1) - O(1)	100.2(4)
C(16)–Sn(1)–O(2)	85.6(4)
C(16)–Sn(1)–O(51)	98.8(4)
C(16)–Sn(1)–O(52)	82.7(4)

4. Supplementary material

Hydrogen coordinates, full list of bond distances and angles and anisotropic displacement parameters. F_o/F_c listing is available from F. Caruso (e-mail: caruso@isc.mlib.cnr.it).

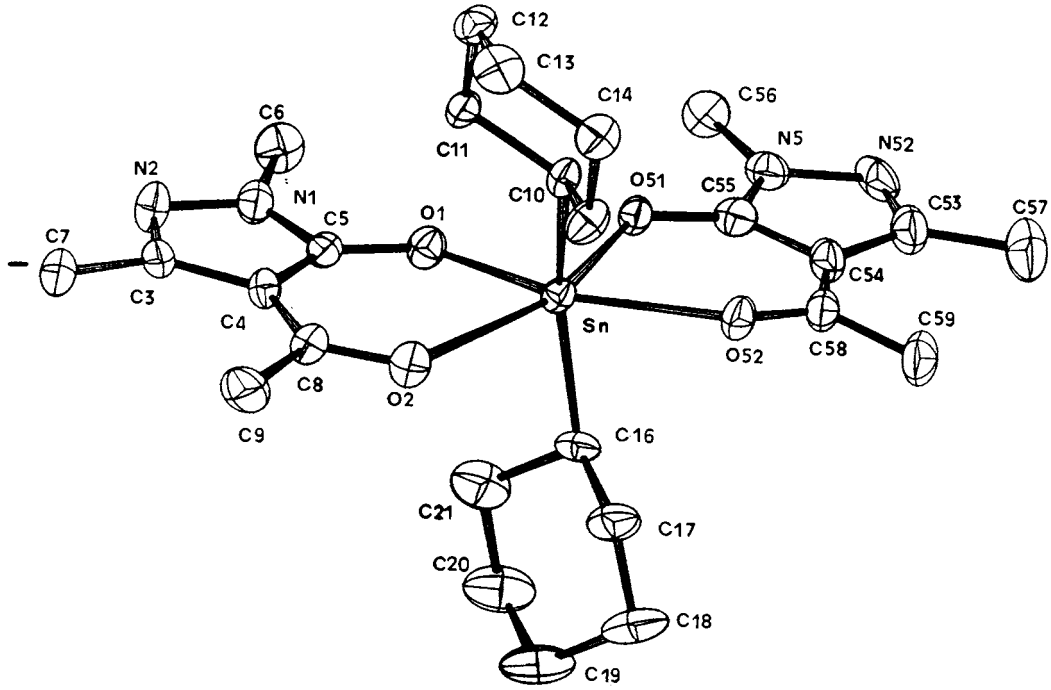

Fig. 8. ORTEP view of the compound $(Q_D)_2SnCy_2$.

Table 8
Selected geometrical data in the coordination sphere for diorganotinbis(β-diketonate) compounds

Compound[a]	Sn–O_p^b (a)	Sn–O_s^c (b)	(b)–(a)	Sn–C	O_p–Sn–O_p	O_s–Sn–O_s	O_p–Sn–O_s (bite)	C–Sn–C	Geometry	Ref.
$Me_2Sn(acac)_2$	2.18(1)			2.14(2)	94(1)		86(1)	180	Octahedral	([5]a)
	2.20(2)									
$Ph_2Sn(Q_{Br})_2$	2.143(7)	2.223(8)	0.08	2.11(1)	91.9(3)	98.6(3)	84.5(4)	173.0(7)	STB	([6]c)
	2.12(1)	2.26(1)	0.14	2.11(2)			85.1(3)			
$Bz_2Sn(Q^{OMe})_2$	2.105(6)	2.359(7)	0.254	2.12(1)	84.1(3)	107.4(2)	83.5(2)	164.5(4)	STB	([6]e)
	2.109(7)	2.329(7)	0.220	2.15(1)			85.0(3)			
$Me_2Sn(Q'')_2$	2.123(4)	2.288(4)	0.165	2.101(8)	82.7(1)	111.5(2)	82.9(2)	162.1(3)	STB	([22]b)
	2.105(5)	2.321(4)	0.216	2.118(7)			83.2(1)			
$Me_2Sn(Q_2^{O\text{-}i\text{-}Pr})$	2.10(1)	2.39(1)	0.29	2.07(2)	82.0(4)	112.7(4)	81.8(4)	157.0(8)	STB	([6]d)
	2.09(1)	2.39(1)	0.30	2.09(2)			83.7(4)			
$Bu_2^nSn(Q')_2$	2.12(2)	2.35(2)	0.23	2.07(2)	79.2(5)	118.7(4)	82.0(4)	154.7(8)	STB	([22]a)
	2.11(2)	2.38(2)	0.27	2.12(2)			80.3(4)			
$Cy_2Sn(Q_D)_2$	2.094(9)	2.42(1)	0.326	2.17(1)	77.8(3)	121.2(3)	80.4(3)	154.6(5)	STB	This work
	2.132(9)	2.405(8)	0.273	2.14(1)			80.5(3)			
$Me_2Sn(Q_{Br})_2$	2.104(4)	2.385(5)	0.281	2.097(8)	75.5(2)	126.7(2)	78.5(2)	154.5(3)	STB	([6]b)
	2.099(4)	2.436(5)	0.337	2.099(8)			79.5(2)			
$Me_2Sn(Q')_2$	2.104(3)	2.337(4)	0.233	2.095(8)	77.2(1)	121.6(1)	80.9(1)	153.3(3)	STB	([6]a)
	2.103(4)	2.412(4)	0.309	2.090(8)			80.7(1)			
$Bu_2^tSn(Q')_2$	2.145(5)	2.381(7)	0.236	2.20(1)	74.1(2)	127.4(2)	79.3(2)	150.0(5)	STB	[1]
	2.135(6)	2.461(6)	0.326	2.20(2)			79.8(2)			

[a] acac = pentane-2,4-dionato; Q′ = 1-phenyl-3-methyl-4-benzoylpyrazolon-5-ato; Q″ = 1-phenyl-3-methyl-4-acetylpyrazolon-5-ato; Q_{Br} = 1-phenyl-3-methyl-4-*p*-bromobenzoylpyrazolon-5-ato; $Q^{O\text{-}i\text{-}Pr}$ = 1-phenyl-3-methyl-4-isopropoxycarbonylpyrazolon-5-ato; Q^{OMe} = 1-phenyl-3-methyl-4-methoxycarbonyl pyrazolon-5-ato; Q_D = 1,3-dimethyl-4-acetylpyrazolon-5-ato.
[b] O_p, primary bond.
[c] O_s, secondary bond.

Table 9
Summary of crystal data

Formula	$C_{24}H_{40}N_4O_4Sn$
Formula weight	567.30
a (Å)	34.398(10)
b (Å)	18.242(7)
c (Å)	9.248(3)
β (°)	97.81(3)
Volume (A^3)	5749(3)
Space group	$C2/c$
Z	8
Crystal dimensions (mm)	$0.35 \times 0.20 \times 0.20$
Density calc. (g cm^{-3})	1.311
Temperature	298 K
$F(000)$	2352
μ (cm^{-1})	9.296
Radiation	Mo–Kα
Data collection mode	ω
Scan speed (° min^{-1})	2
Scan range (°)	0.6
Background counts	1/4 of scan time at the end of scan range
2θ range (°)	3–56
Reflections refined	2886
Final no. variables	316
R_f, R_w	0.059, 0.080

Acknowledgements

Financial support by Università degli Studi di Camerino, Consiglio Nazionale delle Ricerche C.N.R.-Rome, Research Committee and URSI program at Vassar College.

References

[1] C. Pettinari, G. Rafaiani, G. Gioia Lobbia, A. Lorenzotti, F. Bonati, B. Bovio, J. Organomet. Chem. 405 (1991) 75.
[2] S. Miyazaki, H. Mukai, S. Umetani, S. Kihara, M. Matsui, Inorg. Chem. 28 (1989) 3014.
[3] K. Venkataraman, in: The Chemistry of Synthetic Dyes, vol. 1, Academic Press, New York, 1952.
[4] M.F. Mahon, K.C. Molloy, B.A. Omotowa, M.A. Mesubi, J. Organomet. Chem. 525 (1996) 239.
[5] (a) G.A. Miller, E.O. Schlemper, Inorg. Chem. 12 (1977) 677. (b) G. Poli, C.J. Cheer, W.H. Nelson, J. Organomet. Chem. 306 (1986) 347.
[6] (a) B. Bovio, A. Cingolani, F. Marchetti, C. Pettinari, J. Organomet. Chem. 458 (1993) 39. (b) C. Pettinari, F. Marchetti, D. Leonesi, M. Rossi, F. Caruso, J. Organomet. Chem. 483 (1994) 123. (c) F. Caruso, D. Leonesi, F. Marchetti, E. Rivarola, M. Rossi, V. Tomov, C. Pettinari, J. Organomet. Chem. 519 (1996) 9. (d) C. Pettinari, F. Marchetti, A. Gregori, A. Cingolani, J. Tanski, M. Rossi, F. Caruso, Inorg. Chim. Acta 257 (1997) 37. (e) C. Pettinari, F. Marchetti, A. Cingolani, A. Lorenzotti, E. Mundorff, M. Rossi, F. Caruso, Inorg. Chim. Acta 262 (1997) 33.
[7] D.L. Kepert, Prog. Inorg. Chem. 23 (1977) 1.
[8] E.C. Okafor, B.A. Uzoukwu, Synth. React. Inorg. Met. Org. Chem. 23 and references reported therein.
[9] B.S. Jensen, Acta Chem. Scand. 13 (1959) 1347, 1668, 1890.
[10] D. Searle, P.J. Smith, N.A. Bell, L.A. March, I.W. Nowell, J.D. Donaldson, Inorg. Chim. Acta 162 (1989) 143.
[11] (a) A.J. Crowe, P.J. Smith, Chem. Ind. (1980) 200. (b) A.J. Crowe, P.J. Smith, G. Atassi, Chem. Biol. Interact. 32 (1980) 171. (c) M. Gielen (Ed.), Tin-based Antitumor Drugs, NATO ASI Ser. H. Cell Biology, vol. 37, Brussels, 1989.
[12] C. Pettinari, F. Marchetti, A. Cingolani, C. Marciante, R. Spagna, M. Colapietro, Polyhedron 13 (1994) 939.
[13] K. Nakamoto, Infrared and Raman Spectra of Inorganic and Coordination Compounds, 4th ed., Wiley Interscience, New York, 1986, chap. III, pp. 259–267.
[14] (a) M. McGrady, R.S. Tobias, Inorg. Chem. 3 (1964) 1157. (b) R.W. Jonas, R.C. Fay, Inorg. Chem. 12 (1973) 2599. (c) I. Wharf, D.F. Shiver, Inorg. Chem. 8 (1969) 914. (d) J.R. May, W.R. McWhinnie, R.C. Poller, Spectrochim. Acta 27A (1971) 969. (e) A.L. Smith, Spectrochim. Acta 24A (1967) 695. (f) M.S. Dance, W.R. McWhinnie, R.C. Poller, J. Chem. Soc. Dalton Trans. (1976) 2349. (g) G.K. Sandhu, N.S. Boparoy, J. Organomet. Chem. 411 (1991) 89. (h) F. Huber, M. Vornfield, G. Ruisi, R. Barbieri, Appl. Organomet. Chem. 7 (1993) 243.
[15] B. Wrackmeyer, Annu. Rep. NMR Spectrosc. 16 (1985) 73.
[16] J. Holecec, A. Lycka, Inorg. Chim. Acta 118 (1986) L15.
[17] T.P. Lockhart, W.F. Manders, Inorg. Chem. 25 (1986) 892.
[18] (a) J.A.S. Smith, E.J. Wilkins, J. Chem. Soc. A (1966) 1749. (b) R. Ueeda, Y. Kawasaki, T. Tanaka, R. Okawara, J. Organomet. Chem. 5 (1966) 194. (c) V. Doron, C. Fischer, Inorg. Chem. 6 (1967) 1917. (d) J.W. Faller, A. Davison, Inorg. Chem. 6 (1967) 182. (e) G.E. Glass, R.S. Tobias, J. Organomet. Chem. 15 (1968) 481.
[19] R.O. Day, R.R. Holmes, A. Schmidpeter, K. Stoll, L. Howe, Chem. Ber. 124 (1991) 2443.
[20] A.G. Davies, P.G. Harrison, J.D. Kennedy, T.N. Mitchell, R.J. Puddephatt, W. Ramsay, W. McFarlane, J. Chem. Soc. C (1969) 1136.
[21] W.H. Nelson, Inorg. Chem. 6 (1967) 1509.
[22] (a) S. Saxena, R. Bohra and A.K. Ray, Inorg. Chim. Acta 173 (1990) 191. (b) A. Jain, S. Saxena, R. Bohra, A.K. Ray, Main Group Met. Chem. 18 (1995) 139.
[23] L. Pauling, The Nature of the Chemical Bond, 3rd ed., Cornell Univ. Press, Ithaca, New York, 1960, pp. 260.
[24] K. Sisido, Y. Takedo, Z. Kinugawa, J. Am. Chem. Soc. 83 (1961) 538.
[25] A.I. Vogel, Vogel's Textbook of Practical Organic Chemistry, Longman, Harlow, 1989, chap. 8, p.1150.
[26] M. Camalli, D. Capitani, G. Cascarano, S. Cerrini, G. Giacovazzo, R. Spagna, Caos Program: User guide, 1st Strut. Chim. CNR Monterotondo Stazione, Rome, Italy, 1986.
[27] D.J. Cruickshank, in: J.S. Rollet (Ed.), Computing Methods in Crystallography, Pergamon, Oxford, 1965, pp. 114.
[28] International Tables for X-ray Crystallography, Kynoch, Birmingham, UK, 1974.